Research article

Carbon Future

Efficient catalytic conversion of polyethylene terephthalate to dimethyl terephthalate over mesoporous Beta zeolite supported zinc oxide

Xiaoxue Mu[1,#], Dongquan Lin[1,#], Jian Zhang[1] ✉, Xiaoyuan Qin[1], Jianbin Huang[1], and Feng-Shou Xiao[1,2] ✉

[1] *Beijing Advanced Innovation Center for Soft Matter, Science and Engineering, Beijing University of Chemical Technology, Beijing 100029, China*

[2] *Key Lab of Biomass Chemical Engineering of Ministry of Education, College of Chemical and Biological Engineering, Zhejiang University, Hangzhou 310027, China*

Cite This: *Carbon Future* **2025**, *2*, 9200039

Read Online

ABSTRACT: Methanolysis of polyethylene terephthalate to dimethyl terephthalate is a sustainable route for recycling of polyethylene terephthalate (PET) plastic. Herein, we demonstrate that mesoporous Beta zeolite supported zinc oxide (Zn-Beta-meso) is efficient for methanolysis of polyethylene terephthalate to dimethyl terephthalate, exhibiting ~ 99.9% dimethyl terephthalate yield at 180 °C after reaction for 30 min. Model reactions confirmed that the key step in PET methanolysis was the methanolysis of 2-hydroxyethyl methyl terephthalate to form dimethyl terephthalate, where the highly dispersed zinc species are the active sites for this step. In addition, the Zn-Beta-meso catalyst was active for the methanolysis of various PET substrates. When bottle with pigment, terylene, transparent adhesive tape, and soundproof cotton were applied as the substrates, full PET conversion and higher than 99.0% dimethyl terephthalate yield were obtained.

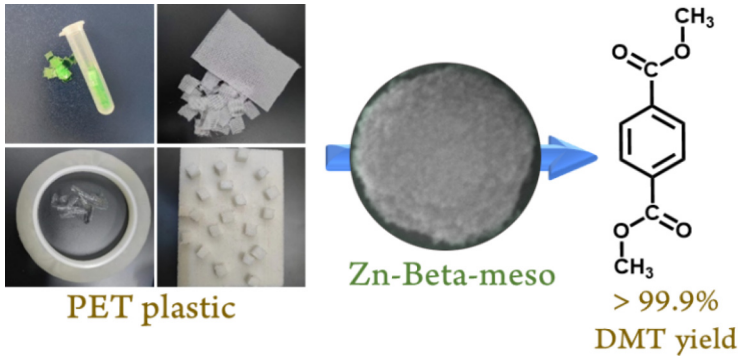

KEYWORDS: mesoporous zeolite, zinc species, polyethylene terephthalate, methanolysis, dimethyl terephthalate

1 Introduction

Polyethylene terephthalate (PET), as a common plastic, has been widely used in the production of vessels, textiles, film, and engineering plastic[1–16]. Worldwide annual PET production has been reported to exceed 31 million metric tons in 2019[7]. However, it has been discovered that used PET plastic can be only transformed into non-degradable microplastics under outdoor conditions, which are harmful to humans and animals[17–19]. Therefore, the recycling of waste PET plastic is an urgent issue that cannot be delayed[20–22]. Although various methods have been developed for PET recycling, one of the most promising routes is direct conversion of PET with methanol to produce dimethyl terephthalate (DMT), which is known as the methanolysis of PET. This method exhibits effective decomposition, and the resulting decomposition products can be directly used for synthesizing new PET[23].

Great efforts have been devoted to the methanolysis of PET[24–30]. Yang and co-workers investigated the methanolysis of PET with supercritical methanol under optimal conditions (9.0–11.0 MPa, 260–270 °C), which achieved a PET degradation efficiency of > 99.9%[28]. However, high energy costs are needed because of the lack of catalysts. Homogeneous catalysts such as metal acetates were reported active in PET methanolysis[31]. However, the homogeneous nature of these metal salts hindered the wide application of the above processes. Alternatively, various heterogeneous solid acid/base catalysts such as metal oxides and zeolites have been developed for this reaction[32, 33]. Among these catalysts, zeolites with abundant acidic sites and rigid microporous channels are promising for PET methanolysis. However, special reactor such as microwave autoclave was necessary because the microporous channels make some active sites unavailable for the large PET molecule[33]. At the same time, heterogeneous zinc-containing catalysts are quite efficient for PET alcoholysis[34]. Therefore, it is reasonable to achieve high PET methanolysis activity through the induction of mesoporous channels and Zn species in zeolites.

Received: December 26, 2024; **Revised:** January 6, 2025
Accepted: February 11, 2025

✉Address correspondence to Jian Zhang, jianzhangbuct@buct.edu.cn; Fengshou Xiao, fsxiao@zju.edu.cn

#Xiaoxue Mu and Dongquan Lin contributed equally to this work.

https://doi.org/10.26599/CF.2025.9200039

Herein, we report the efficient methanolysis of PET by a mesoporous Beta zeolite supported Zn catalyst (Zn-Beta-meso). Due to the presence of abundant mesoporosity and highly dispersed Zn species, the Zn-Beta-meso is quite efficient for PET methanolysis, achieving a conversion rate of 99.9%, with a corresponding yield of 99.9% at 180 °C. Model reactions conclude that the rate-determining step in PET methanolysis is the methanolysis of 2-hydroxyethyl methyl terephthalate (MHET) to form dimethyl terephthalate (DMT) and the Zn species are the active sites in the Zn-Beta-meso catalyst. Additionally, the Zn-Beta-meso catalyst is active for the methanolysis of other kinds of PET such as pigment, terylene, transparent adhesive tape, and soundproof cotton. Full PET conversion and > 99.0% DMT yield were achieved when these PET materials were applied as the reaction substrates.

2 Experimental details

2.1 Materials

Fumed silica (SiO_2, 99.5%), petroleum ether (analytical reagent (AR)), and ethyl acetate ($CH_3COOCH_2CH_3$, AR) were purchased from Aladdin chemical Co., Ltd. Zinc nitrate hexahydrate [$Zn(NO_3)_2{\cdot}6\ H_2O$, AR], sodium aluminate ($NaAlO_2$, commercially pure (CP)), ammonium chloride (NH_4Cl, AR), sodium hydroxide (NaOH, AR), ethylene glycol ($C_2H_6O_2$, AR), and ethanol (AR) were purchased from Sinopharm Chemical Reagent Co., Ltd. O,O'-(Ethane-1,2-diyl)dimethyl diterephthalate (DMT dimer, 98%) was purchased from Shanghai Bide pharmaceutical technology Co., Ltd. DMT (> 99%), terephthalic acid (TPA, > 99%), and bis(2-hydroxyethyl) terephthalate (BHET, > 85%) were purchased from TCI (Shanghai) development Co., Ltd. Methanol (CH_3OH, high-performance liquid chromatography (HPLC)) was purchased from Honeywell (China) Co., Ltd. Hexane (C_6H_{14}, HPLC) and 2-hydroxyethyl methyl terephthalate (MHET, > 97%) were purchased from Shanghai Macklin biochemical Co., Ltd. Isopropanol (i-C_3H_7OH, HPLC) was purchased from J&K scientific Ltd. Polydimethyldiallylammonium chloride (PDADMAC, 20 wt.%) was purchased from Sigma-Aldrich Shanghai trading Co., Ltd. H-Beta-micro (Si/Al = 13), ZSM-5 (Si/Al = 13), and Y (Si/Al = 5) zeolites were purchased from Nankai catalyst factory. SBA-15 (XFNANO XFF01, pore diameter: 7–9 nm, surface area: 550–600 m^2/g) was purchased from Jiangsu Xianfeng Nano Material Technology Co., Ltd.

2.2 Synthesis of catalyst

The H-form mesoporous Beta zeolites (H-Beta-meso) sample was synthesized from PDADMAC as a template reported by our group with a little modification[35]. The synthesis procedures were as follows: 0.080 g of $NaAlO_2$ and 0.278 g of NaOH were dissolved into 12.500 g of water, followed by addition of 0.940 g of fumed silica. After stirring for 24 h under ambient conditions, 2.400 g of PDADMAC was added into the gel. After stirring for another 24 h, the obtained gel was transferred into an autoclave and hydrothermally treated at 180 °C for 10 days. The obtained zeolite was separated by centrifugation, washed with a large amount of water, dried at 80 °C, calcined at 550 °C for 5 h, ion-exchanged with a 1 mol/L NH_4Cl solution at 80 °C for two times, and calcined at 500 °C for 3 h to finally obtain the H-Beta-meso sample.

The Zn-Beta-meso sample was synthesized from an impregnation method. Typically, 0.100 g of H-Beta-meso was added into a solution containing 0.041 g of $Zn(NO_3)_2{\cdot}6H_2O$ and 0.200 g of water. The obtained suspension was ultrasoundly treated for 1 h and aged at ambient temperature overnight. Then, water was evaporated by heating at 80 °C, and the obtained solid was calcined at 550 °C for 5 h to obtain the Zn-Beta-meso catalyst. The ratio of silicon to aluminum (Si/Al) was determined at 12.5 through inductively coupled plasma (ICP) analysis.

The syntheses of the Zn-Beta-micro, Zn-ZSM-5, Zn-Y, and Zn-SBA-15 catalysts were the same as that of the Zn-Beta-meso catalyst except for the replacement of H-Beta-micro with H-Beta-meso.

2.3 Characterizations

Scanning transmission electron microscopy (STEM) images were obtained using a TEM-2100F electron microscope (JEOL, Japan) with an acceleration voltage of 200 kV. Meanwhile, the analysis of elemental distribution was performed on an Oxford Instruments X-Max 80T. X-ray diffraction (XRD) was performed using a Rigaku D/MAX 2550 instrument equipped with a Cu Kα radiation source (λ = 1.5418 Å). ICP-optical emission spectroscopy (ICP-OES) was utilized for determining elemental contents. Before tests, the samples were dissolved with a mixed solution of hydrofluoric (HF) acid and HNO_3. Thermalgravimetric (TG) analysis was conducted under air atmosphere with a heating rate of 10 °C/min. ^{13}C nuclear magnetic resonance (NMR) spectra were acquired using a Bruker Avance 400 spectrometer, with the sample dissolved in dimethyl sulfoxide (DMSO)-d6. Scanning electron microscopy (SEM) images were captured using a Zeiss Supra 55 at an accelerating voltage of 10 kV. The experiments for MHET adsorption Fourier transform infrared (FTIR) spectra were recorded using a VERTEX 70 BRUKER infrared spectrometer equipped with and a high-temperature reaction cell. The 2,4,6-tritert-butylpyridine adsorption FTIR (Py-FTIR) spectra were obtained on the same apparatus[36]: Prior to adsorption, the sample was pressured into wafers and placed into the *in-situ* cell. The wafer was vacuum-treated at 400 °C for 1 h and cooled to 200 °C to collect the background spectra. Subsequently, a tetrahydrofuran solution of 2,4,6-tritert-butylpyridine (80 μL, 0.1 mol/L) was introduced and vacuum treated at 200 °C until steady. All obtained FTIR spectra had been automatically background-subtracted.

2.4 Catalytic methanolysis of PET

The reaction was conducted in a 100 mL stainless steel reactor equipped with a magnetic stirrer and a heating jacket. Before reaction, various forms of PET such as tape, soundproofing material, polyester, and colored plastic bottles were cut into 1 cm × 1 cm squares. These samples were subjected to two rounds of 10-min ultrasonic treatment in anhydrous ethanol and then dried at room temperature before being used in reactions. Typically, 0.150 g of PET, 0.030 g of catalyst, and 20 g of methanol were added into the reactor. The reactor was then charged with 3 MPa of N_2, sealed, and heated to desired reaction temperature. After a certain period of time, the reactor was allowed to rapid cooling by cold water. The solution was then removed by centrifugation to separate the catalyst, reactants, and product solution. PET conversion was calculated by weighting. The filtrate was analyzed using HPLC equipped with a reverse-phase silica gel chromatography column (GL Sciences, INERSTIL SIL-100A 5UM 2.6 × 250 mm) and an ultraviolet (UV) detector (254 nm). A gradient elution method was employed with a mobile phase composed of hexane and isopropanol. The initial flow rate of isopropanol was set at 0.2 mL/min, increased to 0.8 mL/min after 5 min, maintained until

15 min, and then decreased to 0.2 mL/min by 20 min. For hexane, the initial flow rate was 0.6 mL/min, reduced to 0 mL/min after 5 min, maintained for 15 min, and increased back to 0.6 mL/min by 20 min. DMT, MHET, and DMT dimer were quantified using an external standard method. The equations for calculating DMT, MHET, and DMT dimer yields were in the following Eqs. (1)–(3)

$$\text{Yield of DMT} = \left(\frac{\text{weight of DMT} \times \text{relative molecular mass of PET}}{\text{weight of PET} \times \text{relative molecular mass of DMT}}\right) \times 100\% \quad (1)$$

$$\text{Yield of MHET} = \left(\frac{\text{weight of MHET} \times \text{relative molecular mass of PET}}{\text{weight of PET} \times \text{relative molecular mass of MHET}}\right) \times 100\% \quad (2)$$

$$\text{Yield of DMT dimer} = \left(\frac{2 \times \text{weight of DMT dimer} \times \text{relative molecular mass of PET}}{\text{weight of PET} \times \text{relative molecular mass of DMT dimer}}\right) \times 100\% \quad (3)$$

For the calculation of PET conversion, the dried solids obtained by centrifugation were weighed, and the amount of added catalyst was subtracted to determine the recovered PET after the reaction. The equation for calculating conversion of PET was in the following Eq. (4)

$$\text{PET conversion} = \left(1 - \frac{\text{weight of recovered PET}}{\text{weight of feeding PET}}\right) \times 100\% \quad (4)$$

The recyclability of the catalyst was studied by separating the catalyst after reaction, washing with ethanol, drying under 80 °C, and used for the next run. After recycling for 4 times, the used catalyst was calcined at 550 °C for 5 h in flowing O_2 (25 mL/min) to remove the coke species and used for the next run.

3 Results and discussion

3.1 Catalyst characterization and methanolysis of PET to DMT

For the preparation of Zn-Beta-meso catalyst, mesoporous Beta zeolite (Beta-meso) was firstly synthesized using PDADMAC as a dual-function template[35]. After ion-exchange with NH_4Cl solution and calcination, H-Beta-meso was obtained. By loading Zn species on H-Beta-meso from an impregnation method, Zn-Beta-meso was finally prepared (see Section 2.2 for detailed information). **Fig. 1a** displays representative XRD patterns of ZnO and H-Beta-meso before and after Zn loading. Both H-Beta-meso and Zn-Beta-meso showed characteristic peaks associated with *BEA zeolite structure[35, 37], while the peaks (31.7°, 34.4°, and 36.2°) related to ZnO phase completely disappeared. These results suggest that the Zn species are highly dispersed on the Zn-Beta-meso sample (Fig. 1a). As shown in Supplementary Fig. S1, the Zn-Beta-meso exhibited peaks at 1045.0 and 1022.2 eV on the Zn 2p X-ray photoelectron spectroscopy (XPS) spectrum, which are associated with Zn^{2+} species[38, 39]. This result confirms that the Zn species in the Zn-Beta-meso should be zinc oxide. Fig. 1b shows N_2-sorption isotherms of various catalysts. The H-Beta-meso and Zn-Beta-meso samples exhibited steep steps in the P/P_0 ranges of both less than 0.05 and 0.4–0.8 (Fig. 1b), indicating the presence of both microporosity and mesoporosity[35, 40]. After loading the Zn species, the Zn-Beta-meso had lower surface area and pore volume than those of H-Beta-meso (Supplementary Table S1), suggesting that these Zn species might be highly dispersed into these pores, which is in good agreement with those obtained from the XRD patterns. Supplementary Fig. S2 gives SEM images of Zn-Beta-meso and H-Beta-meso samples, exhibiting similar spherical particles with particle sizes of 600–700 nm. **Fig. 2** shows the STEM image and elemental mappings of Zn-meso-Beta, indicating that Zn species are highly dispersed on the zeolite support, which is well consistent with the XRD results (Fig. 1a).

Fig. 3a shows possible reaction route and performances in the methanolysis of PET over the Zn-Beta-meso. As expected, the Zn-Beta-meso was efficient for this reaction, giving > 99% PET conversion and > 99% DMT yield (Fig. 3b) under optimized conditions (Supplementary Figs. S3 and S4 and Table S2). This value is comparable to the previously-reported excellent PET methanolysis catalysts (Supplementary Table S3). In contrast, the DMT yields of H-Beta-meso and ZnO samples were < 1% and 72%, respectively (Fig. 3b). In addition, Zn species on conventional Beta (Zn-Beta-micro), ZSM-5 (Zn-ZSM-5), and Y (Zn-Y) zeolites had the DMT yields at 61%, 81%, and 86%, respectively (Fig. 3b and

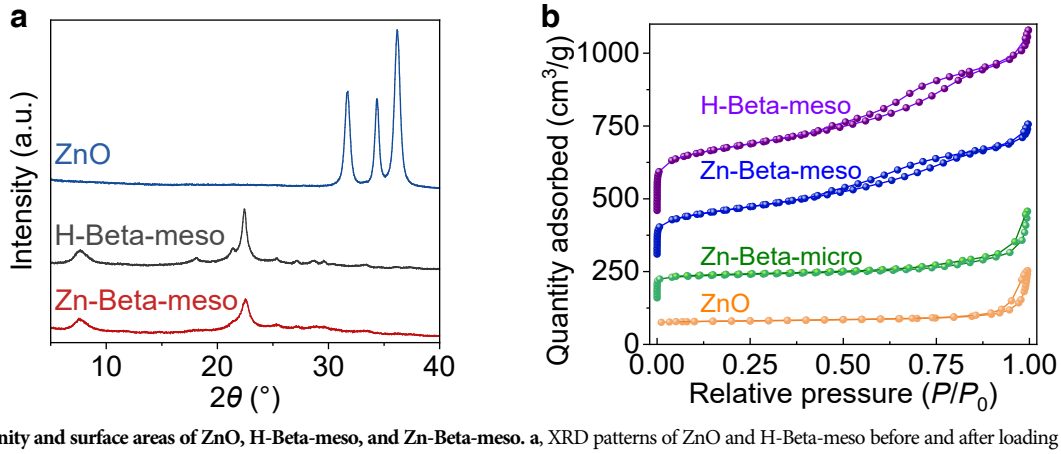

Fig. 1. Crystallinity and surface areas of ZnO, H-Beta-meso, and Zn-Beta-meso. a, XRD patterns of ZnO and H-Beta-meso before and after loading Zn species. **b**, N_2-sorption isotherms of ZnO, Zn-Beta-micro, and H-Beta-meso before and after loading Zn species.

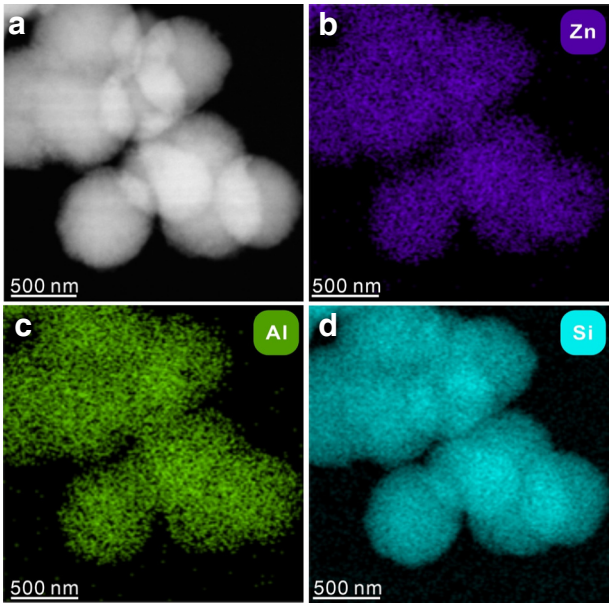

Fig. 2. SEM characterization of Zn-Beta-meso sample. a–d, STEM image (a) and corresponding elemental mappings of Zn (b), Al (c), and Si (d) of the Zn-Beta-meso sample.

Supplementary Fig. S6). These results suggest that both Zn species and mesoporosity (Supplementary Table S4) are critical for the contribution of DMT yields. Furthermore, Zn-Beta-meso is also active for other kinds of PET materials. Full PET conversion and high DMT yield at 99%, > 99%, 99%, > 99% were achieved when bottle with pigment, terylene, transparent adhesive tape, and soundproof cotton were applied as the reaction substrates, respectively (Supplementary Fig. S7). These results also showed that the Zn-Beta-meso was highly efficient for the PET methanolysis (Supplementary Fig. S7).

The Zn-Beta-meso catalyst is recyclable. After reaction, the catalyst can be separated by filtration, washed with methanol, and used for the next run (Fig. 3c and Supplementary Fig. S8). The Zn-Beta-meso exhibited DMT yields at 99% and 99% in the second and third run, respectively, which are comparable to the fresh one (Fig. 3c). However, the DMT yield of the fourth run was decreased to 91% (Fig. 3c). As observed from STEM image and elemental mappings of the used Zn-Beta-meso, it was shown that the particle sizes and elemental distribution of the catalyst were well remained (Supplementary Fig. S9). Therefore, the reduction of the DMT yield might be related to the coke formation, as evidenced by TG curve of the Zn-Beta-meso after used for 4 times. It can be clearly observed that there was a mass loss of 8.4 wt.% in the temperature higher than 300 °C (Supplementary Fig. S10)[41]. After calcination at 550 °C for 5 h in air to remove the coke of the catalyst, the DMT yield of the fifth run was back to ~ 99% (Fig. 3c), supporting the coke formation of the catalyst in the fourth run. Additionally, Zn species might leach during reaction. As shown in Supplementary Table S1, the spent Zn-Beta-meso exhibited Zn loading amount at 8.6 wt.%, which is lower than that (9.0 wt.%) of the fresh one. These results support leaching of Zn species during reaction. In addition, we performed hot filtration to remove the Zn-Beta-meso catalyst to test if the leached Zn species is active for PET methanolysis. As shown in Supplementary Fig. S11, a DMT yield of 85% was achieved after reaction for 5 min. After hot filtration and reaction for another 25 min, a comparable DMT yield of 85% was obtained, showing that the possible leached Zn species was inactive for PET methanolysis or that the leached Zn species was little.

3.2 Key step in PET methanolysis

It has been reported that the PET methanolysis generally involves several steps (Supplementary Fig. S12)[42]. Initially, long-chain PET molecules undergo methanol-mediated reactions, forming short-chain PET molecules (methanolysis of terminal and internal ester

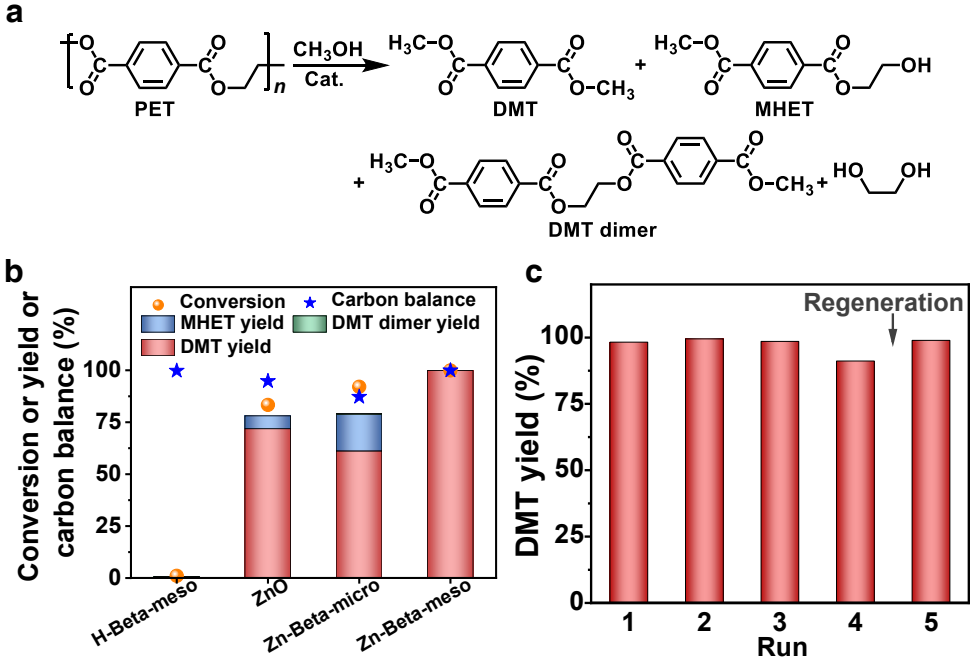

Fig. 3. Catalytic methanolysis of PET over various Zn catalysts. a, Possible reaction products for PET methanolysis. **b**, PET conversion, yields of DMT, MHET, DMT dimer, and carbon balance for PET methanolysis over various catalysts. Reaction conditions: 0.15 g of PET, 0.03 g of catalyst, 20 g of methanol, 3 MPa of N_2 (room temperature), 30 min, and 180 °C. **c**, Recyclable tests over the Zn-Beta-meso catalyst in PET methanolysis.

groups). Subsequently, these short-chain PET molecules were further transformed into DMT dimers, which then gradually formed DMT products through an equilibrium with MHET[43–45]. To compare the methanolysis of ester bonds at different positions, BHET dimer with both terminal and internal ester groups was synthesized and its ^{13}C NMR spectrum is shown in Supplementary Fig. S13. Methanolysis of BHET dimer over the Zn-Beta-meso was performed as a model reaction to simulate reaction mechanism for PET methanolysis (**Fig. 4**a). Fig. 4b shows the product distribution as a function of reaction time. After reaction for 15 min, the Zn-Beta-meso exhibited MHET and DMT dimer yields at 22.2% and 2.7%, respectively (Fig. 4b). This phenomenon suggests that the methanolysis of terminal and internal ester groups proceeds simultaneously. With prolonging reaction time, the MHET first increased and then decreased. The MHET yields were 29.4%, 34.5%, and 21.0% after reaction for 30, 60, and 90 min, respectively (Fig. 4b). Interestingly, the DMT yield significantly increased when MHET yield decreased with prolonging reaction time. The DMT yields were 6.4%, 27.2%, and 82.9% after reaction for 30, 60, and 90 min, respectively (Fig. 4b). These results suggest that DMT was mainly resulted from the methanolysis of MHET. Furthermore, the reaction rate constants for the methanolysis of BHET dimer, DMT dimer, and MHET were tested to determine the rates for the methanolysis of terminal, internal, and MHET ester groups. As shown in Fig. 4c, the reaction rate constants for BHET dimer, DMT dimer, and MHET were 0.028, 0.037, and 0.018 min^{-1}, respectively. The slowest reaction rate for conversion of MHET to DMT indicates that the methanolysis of MHET is a key step for PET methanolysis[44].

3.3 Insights into the catalytic active sites

Based on the aforementioned results and previous studies, it is suggested the mechanism of PET methanolysis over the Zn-Beta-meso catalysts, as shown in Supplementary Fig. S12. At first, the long-chain PET molecules were attacked by methanol from the end of chain, then conducting stepwise ester-exchange reactions inward, resulting in the formation of numerous PET short chains, which were then transformed into MHET. Subsequently, further ester-exchange reactions lead to the production of the final product of DMT from MHET. Due to relatively low concentration, the generated ethylene glycol does not undergo ester exchange to form BHET. Consequently, this substance remains undetectable during the reaction process (Fig. 3b).

Then, the catalytic active sites for MHET methanolysis were detected. It has been reported that acidic sites might be active for the methanolysis[33]. Considering the bulky molecules of the long PET chain, the reaction should occur on the external acidic sites of the Zn-Beta-meso samples. To quantify the relationship between catalytic activity and external acidic concentration, we performed *in-situ* FTIR spectra of 2,4,6-tritert-butylpyridine on Zn-Beta-meso catalysts with different Zn loadings[36]. Notably, these Zn-Beta-meso catalysts exhibited comparable acidic sites on the external surface (Supplementary Fig. S14). Because of quite different catalytic performances in the methanolysis of MHET, similar acidic sites on the external surface of these catalysts should not be a major factor for the PET methanolysis. As Zn specie is active for the methanolysis of PET, the reaction rate as a function of Zn loading amounts over Zn-Beta-meso with different Zn loading amounts was studied (**Fig. 5**). Interestingly, dependence of the activities in methanolysis of PET on Zn loading in the Zn-Beta-meso catalysts exhibited a linear relationship (Fig. 5), meaning that the Zn species should be major active sites for the PET methanolysis.

4 Conclusions

In this work, we reported preparation of zinc species supported on mesoporous Beta zeolite from a simple impregnation. The resulting

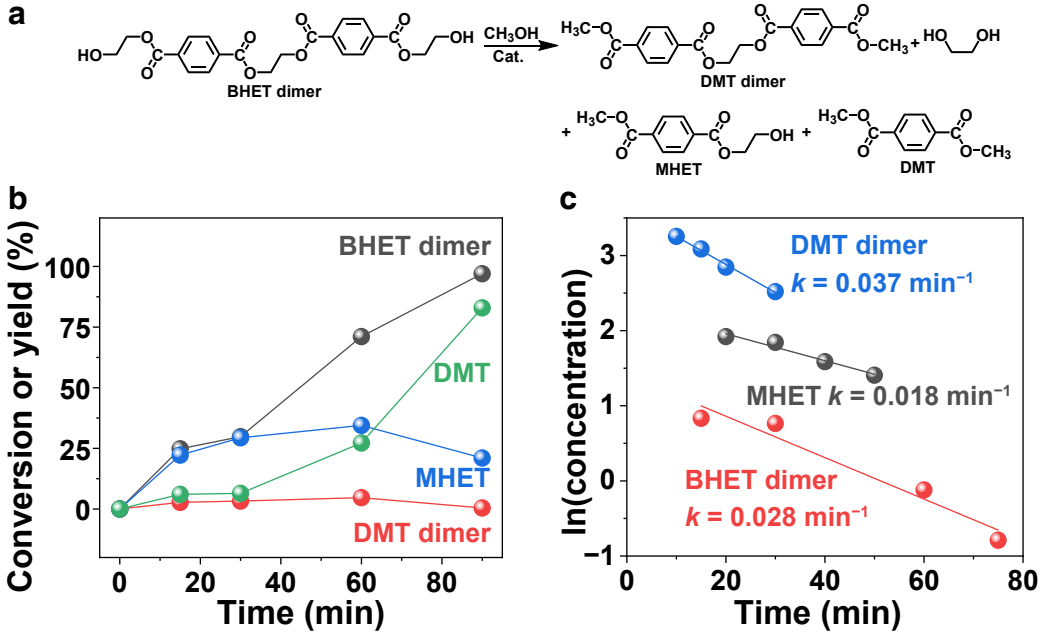

Fig. 4. Kinetic studies for the methanolysis of PET over the Zn-Beta-meso catalyst. a, Possible reaction products for the methanolysis of BHET dimer. **b**, Dependence of BHET dimer conversion and yields of DMT, MHET, and DMT as a function of reaction time in BHET dimer methanolysis over the Zn-Beta-meso catalyst. Reaction conditions: 0.01 g of BHET dimer, 0.001 g of catalyst, 5 g of methanol, 5 g of methanol, 3 MPa of N_2 (room temperature), and 180 °C. **c**, Concentration of DMT dimer, MHET, and BHET dimer as a function of reaction time over the Zn-Beta-meso catalyst. Reaction conditions: 0.01 g of substrate, 0.001 g of catalyst, 5 g of methanol, 3 MPa of N_2 (room temperature), and 180 °C.

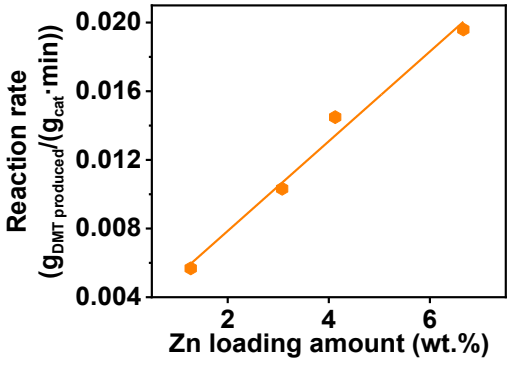

Fig. 5. The relationship between reaction rate and Zn loading in the key step of PET methanolysis.

Zn-Beta-meso catalyst was efficient for the methanolysis of PET, achieving about 99.9% DMT yield at 180 °C after reaction for 30 min, outperforming other Zn-containing catalysts. By employing the methanolysis of BHET dimer as a model, it was observed that the key step in PET methanolysis was the methanolysis of MHET to form DMT, where the Zn species are major active sites. In addition, the Zn-Beta-meso catalyst was active for the methanolysis of various PET substrates. When bottle with pigment, terylene, transparent adhesive tape, and soundproof cotton were applied as the substrates, full PET conversion and DMT yield higher than 99.0% were obtained. This work might be helpful for the development of efficient heterogeneous catalysts for PET methanolysis in the future.

References

[1] Zhang, F.; Zeng, M. H.; Yappert, R. D.; Sun, J. K.; Lee, Y. H.; LaPointe, A. M.; Peters, B.; Abu-Omar, M. M.; Scott, S. L. Polyethylene upcycling to long-chain alkylaromatics by tandem hydrogenolysis/aromatization. *Science* **2020**, *370*, 437–441.

[2] Jing, Y. X.; Wang, Y. Q.; Furukawa, S.; Xia, J.; Sun, C. Y.; Hülsey, M. J.; Wang, H. F.; Guo, Y.; Liu, X. H.; Yan, N. Towards the circular economy: Converting aromatic plastic waste back to arenes over a Ru/Nb_2O_5 catalyst. *Angew. Chem., Int. Ed.* **2021**, *60*, 5527–5535.

[3] Goh, X. Y.; Guo, K. T.; Nguyen, L. T.; Ong, R. H.; Duong, H. M. Fabrication and properties of polyethylene terephthalate (PET) aerogel composites from plastic bottle waste. *Mater. Today Commun.* **2023**, *37*, 107625.

[4] Liu, S. B.; Kots, P. A.; Vance, B. C.; Danielson, A.; Vlachos, D. G. Plastic waste to fuels by hydrocracking at mild conditions. *Sci. Adv.* **2021**, *7*, eabf8283.

[5] Tennakoon, A.; Wu, X.; Paterson, A. L.; Patnaik, S.; Pei, Y. C.; LaPointe, A. M.; Ammal, S. C.; Hackler, R. A.; Heyden, A.; Slowing, I. I. et al. Catalytic upcycling of high-density polyethylene via a processive mechanism. *Nat. Catal.* **2020**, *3*, 893–901.

[6] Kratish, Y.; Marks, T. J. Efficient polyester hydrogenolytic deconstruction via tandem catalysis. *Angew. Chem., Int. Ed.* **2022**, *61*, e202112576.

[7] Rahimi, A.; García, J. M. Chemical recycling of waste plastics for new materials production. *Nat. Rev. Chem.* **2017**, *1*, 0046.

[8] Shi, R.; Liu, K. S.; Liu, F. L.; Yang, X.; Hou, C. C.; Chen, Y. Electrocatalytic reforming of waste plastics into high value-added chemicals and hydrogen fuel. *Chem. Commun.* **2021**, *57*, 12595–12598.

[9] Imran, M.; Kim, B. K.; Han, M.; Cho, B. G.; Kim, D. H. Sub- and supercritical glycolysis of polyethylene terephthalate (PET) into the monomer bis(2-hydroxyethyl) terephthalate (BHET). *Polym. Degrad. Stab.* **2010**, *95*, 1686–1693.

[10] Liang, X.; Wang, M.; Ma, D. One-pot conversion of polyester and carbonate into formate without external H_2. *J. Am. Chem. Soc.* **2024**, *146*, 2711–2717.

[11] Xue, R.; Qiu, C. H.; Zhou, X. L.; Cheng, Y.; Zhang, Z.; Zhang, Y.; Schröder, U.; Bornscheuer, U. T.; Dong, W. L.; Wei, R. et al. Enzymatic upcycling of PET waste to calcium terephthalate for battery anodes. *Angew. Chem., Int. Ed.* **2024**, *63*, e202313633.

[12] Ma, F. H.; Li, Z. Q.; Hu, R. M.; Wang, Z. Q.; Wang, J. P.; Li, J. K.; Nie, Y.; Zheng, Z. K.; Jiang, X. C. Electrocatalytic waste-treating-waste strategy for concurrently upgrading of polyethylene terephthalate plastic and CO_2 into value-added formic acid. *ACS Catal.* **2023**, *13*, 14163–14172.

[13] Cao, R. C.; Zhang, M. Q.; Jiao, Y. C.; Li, Y. C.; Sun, B.; Xiao, D. Q.; Wang, M.; Ma, D. Co-upcycling of polyvinyl chloride and polyesters. *Nat. Sustain.* **2023**, *6*, 1685–1692.

[14] Hu, Y.; Zhang, S. Y.; Xu, J. F.; Liu, Y.; Yu, A. A.; Qian, J.; Xie, Y. J. Highly efficient depolymerization of waste polyesters enabled by transesterification/hydrogenation relay under mild conditions. *Angew. Chem. Int. Ed.* **2023**, *62*, e202312564.

[15] Zhang, S. B.; Hu, Q. K.; Zhang, Y. X.; Guo, H. Y.; Wu, Y. F.; Sun, M. Z.; Zhu, X. S.; Zhang, J. G.; Gong, S. Y.; Liu, P. et al. Depolymerization of polyesters by a binuclear catalyst for plastic recycling. *Nat. Sustain.* **2023**, *6*, 965–973.

[16] Pham, D. D.; Cao, A. N. T.; Kumar, P. S.; Nguyen, T. B.; Nguyen, H. T.; Phuong, P. T. T.; Nguyen, D. L. T.; Nabgan, W.; Trinh, T. H.; Vo, D. V. N. et al. Insight the influence of the catalyst basicity on glycolysis behavior of Polyethylene terephthalate (PET). *Chem. Eng. Sci.* **2023**, *282*, 119356.

[17] Allen, S.; Allen, D.; Phoenix, V. R.; Le Roux, G.; Jiménez, P. D.; Simonneau, A.; Binet, S.; Galop, D. Atmospheric transport and deposition of microplastics in a remote mountain catchment. *Nat. Geosci.* **2019**, *12*, 339–344.

[18] Thompson, R. C.; Olsen, Y.; Mitchell, R. P.; Davis, A.; Rowland, S. J.; John, A. W. G.; Mcgonigle, D.; Russell, A. E. Lost at sea: Where is all the plastic. *Science* **2004**, *304*, 838.

[19] Bai, S. L.; Zhao, Y. B.; Sun, J. H.; Tian, Y.; Luo, R. X.; Li, D. Q.; Chen, A. F. Ultrasensitive room temperature NH_3 sensor based on a graphene-polyaniline hybrid loaded on PET thin film. *Chem. Commun.* **2015**, *51*, 7524–7527.

[20] Barnard, E.; Arias, J. J. R.; Thielemans, W. Chemolytic depolymerisation of PET: A review. *Green Chem.* **2021**, *23*, 3765–3789.

[21] Benyathiar, P.; Kumar, P.; Carpenter, G.; Brace, J.; Mishra, D. K. Polyethylene terephthalate (PET) bottle-to-bottle recycling for the beverage industry: A review. *Polymers* **2022**, *14*, 2366.

[22] Ellis, L. D.; Rorrer, N. A.; Sullivan, K. P.; Otto, M.; McGeehan, J. E.; Román-Leshkov, Y.; Wierckx, N.; Beckham, G. T. Chemical and biological catalysis for plastics recycling and upcycling. *Nat. Catal.* **2021**, *4*, 539–556.

[23] Weckhuysen, B. M. Creating value from plastic waste. *Science* **2020**, *370*, 400–401.

[24] Akhbarizadeh, R.; Dobaradaran, S.; Torkmahalleh, M. A.; Saeedi, R.; Aibaghi, R.; Ghasemi, F. F. Suspended fine particulate matter ($PM_{2.5}$), microplastics (MPs), and polycyclic aromatic hydrocarbons (PAHs) in air: Their possible relationships and health implications. *Environ. Res.* **2021**, *192*, 110339.

[25] Kim, S. W.; Waldman, W. R.; Kim, T. Y.; Rillig, M. C. Effects of different microplastics on nematodes in the soil environment: Tracking the extractable additives using an ecotoxicological approach. *Environ. Sci. Technol.* **2020**, *54*, 13868–13878.

[26] Imran, M.; Kim, D. H.; Al-Masry, W. A.; Mahmood, A.; Hassan, A.; Haider, S.; Ramay, S. M. Manganese-, cobalt-, and zinc-based mixed-oxide spinels as novel catalysts for the chemical recycling of poly(ethylene terephthalate) via glycolysis. *Polym. Degrad. Stab.* **2013**, *98*, 904–915.

[27] Lalhmangaihzuala, S.; Laldinpuii, Z. T.; Khiangte, V.; Lallawmzuali, G.; Thanhmingliana; Vanlaldinpuia, K. Orange peel ash coated Fe_3O_4 nanoparticles as a magnetically retrievable catalyst for glycolysis and methanolysis of PET waste. *Adv. Powder Technol.* **2023**, *34*, 104076.
[28] Yang, Y.; Lu, Y. J.; Xiang, H. W.; Xu, Y. Y.; Li, Y. W. Study on methanolytic depolymerization of PET with supercritical methanol for chemical recycling. *Polym. Degrad. Stab.* **2002**, *75*, 185–191.
[29] Bartolome, L.; Imran, M.; Lee, K. G.; Sangalang, A.; Ahn, J. K.; Kim, D. H. Superparamagnetic γ-Fe_2O_3 nanoparticles as an easily recoverable catalyst for the chemical recycling of PET. *Green Chem.* **2014**, *16*, 279–286.
[30] Du, J. T.; Sun, Q.; Zeng, X. F.; Wang, D.; Wang, J. X.; Chen, J. F. ZnO nanodispersion as pseudohomogeneous catalyst for alcoholysis of polyethylene terephthalate. *Chem. Eng. Sci.* **2020**, *220*, 115642.
[31] Kurokawa, H.; Ohshima, M. A.; Sugiyama, K.; Miura, H. Methanolysis of polyethylene terephthalate (PET) in the presence of aluminium tiisopropoxide catalyst to form dimethyl terephthalate and ethylene glycol. *Polym. Degrad. Stab.* **2003**, *79*, 529–533.
[32] Tang, S. X.; Li, F.; Liu, J. D.; Guo, B.; Tian, Z. N.; Lv, J. H. MgO/NaY as modified mesoporous catalyst for methanolysis of polyethylene terephthalate wastes. *J. Environ. Chem. Eng.* **2022**, *10*, 107927.
[33] Kang, M. J.; Yu, H. J.; Jegal, J.; Kim, H. S.; Cha, H. G. Depolymerization of PET into terephthalic acid in neutral media catalyzed by the ZSM-5 acidic catalyst. *Chem. Eng. J.* **2020**, *398*, 125655.
[34] Cao, J. J.; Lin, Y. H.; Jiang, W.; Wang, W.; Li, X. D.; Zhou, T. P.; Sun, P.; Pan, B. C.; Li, A. M.; Zhang, Q. X. Mechanism of the significant acceleration of polyethylene terephthalate glycolysis by defective ultrathin ZnO nanosheets with heteroatom doping. *ACS Sustain. Chem. Eng.* **2022**, *10*, 5476–5488.
[35] Zhu, J.; Zhu, Y. H.; Zhu, L. K.; Rigutto, M.; Van Der Made, A.; Yang, C. G.; Pan, S. X.; Wang, L.; Zhu, L. F.; Jin, Y. Y. et al. Highly mesoporous single-crystalline zeolite Beta synthesized using a nonsurfactant cationic polymer as a dual-function template. *J. Am. Chem. Soc.* **2014**, *136*, 2503–2510.
[36] Beutel, T. W.; Willard, A. M.; Lee, C.; Martinez, M. S.; Dugan, R. Probing external Brønsted acid sites in large pore zeolites with infrared spectroscopy of adsorbed 2,4,6-tri-tert-butylpyridine. *J. Phys. Chem. C* **2021**, *125*, 8518–8532.
[37] Mahalakshmi, M.; Priya, S. V.; Arabindoo, B.; Palanichamy, M.; Murugesan, V. Photocatalytic degradation of aqueous propoxur solution using TiO_2 and Hβ zeolite-supported TiO_2. *J. Hazard. Mater.* **2009**, *161*, 336–343.
[38] Zhao, D.; Guo, K.; Han, S. L.; Doronkin, D. E.; Lund, H.; Li, J. S.; Grunwaldt, J. D.; Zhao, Z.; Xu, C. M.; Jiang, G. Y. et al. Controlling reaction-induced loss of active sites in ZnO_x/silicalite-1 for durable nonoxidative propane dehydrogenation. *ACS Catal.* **2022**, *12*, 4608–4617.
[39] Song, S. J.; Yang, K.; Zhang, P.; Wu, Z. J.; Li, J.; Su, H.; Dai, S.; Xu, C. M.; Li, Z. X.; Liu, J. et al. Silicalite-1 stabilizes Zn-hydride species for efficient propane dehydrogenation. *ACS Catal.* **2022**, *12*, 5997–6006.
[40] Liao, Y. C.; Liao, F. L.; Chang, W. K.; Wang, S. L. A zeolitic organo-metallophosphate hybrid material with bimodal porosity. *J. Am. Chem. Soc.* **2004**, *126*, 1320–1321.
[41] Arslan, M. T.; Qureshi, B. A.; Gilani, S. Z. A.; Cai, D. L.; Ma, Y. H.; Usman, M.; Chen, X.; Wang, Y.; Wei, F. Single-step conversion of H_2-deficient syngas into high yield of tetramethylbenzene. *ACS Catal.* **2019**, *9*, 2203–2212.
[42] Al-Sabagh, A. M.; Yehia, F. Z.; Eissa, A. M. F.; Moustafa, M. E.; Eshaq, G.; Rabie, A. M.; ElMetwally, A. E. Cu- and Zn-acetate-containing ionic liquids as catalysts for the glycolysis of poly (ethylene terephthalate). *Polym. Degrad. Stab.* **2014**, *110*, 364–377.
[43] Genta, M.; Iwaya, T.; Sasaki, M.; Goto, M.; Hirose, T. Depolymerization mechanism of poly(ethylene terephthalate) in supercritical methanol. *Ind. Eng. Chem. Res.* **2005**, *44*, 3894–3900.
[44] Liu, Q. L.; Li, R. S.; Fang, T. Investigating and modeling PET methanolysis under supercritical conditions by response surface methodology approach. *Chem. Eng. J.* **2015**, *270*, 535–541.
[45] Ma, M. Y.; Wang, S.; Liu, Y.; Yu, H. L.; Yu, S. T.; Ji, C. C.; Li, H. Y.; Nie, G. K.; Liu, S. W. Insights into the depolymerization of polyethylene terephthalate in methanol. *J. Appl. Polym. Sci.* **2022**, *139*, e52814.

Data availability

All data needed to support the conclusions in the paper are presented in the manuscript and the Supplementary Information. Additional data related to this paper may be requested from the corresponding author upon request.

Acknowledgements

This work was supported by the National Natural Science Foundation of China (No. 22272007) and the Fundamental Research Funds for the Central Universities (No. XK2023-12).

Author contributions

X. X. M.: investigation, formal analysis, data curation, conceptualization, and visualization. D. Q. L.: investigation, formal analysis, data curation, conceptualization, and visualization. J. Z.: writing – original draft, formal analysis, data curation, conceptualization, funding acquisition, and supervision. X. Y. Q.: investigation and formal analysis. J. B. H.: investigation. F.-S. X.: writing – review and editing, conceptualization, and supervision.

Competing interests

The authors have no competing interests to declare that are relevant to this article.

Use of AI statement

None.

Additional information

Supplementary Information The online version contains supplementary material available at https://doi.org/10.26599/CF.2025.9200039.